JOURNAL OF GUIDANCE, CONTROL, AND DYNAMICS
Vol. 19, No. 3, May–June 1996

Flexible-Body Dynamics Modeling of a Vehicle Moving on the Rails of a Structure

Achille Messac*
Northeastern University, Boston, Massachusetts 02115

The problem of dynamics modeling of a flexible structure that moves on the surface of another flexible structure is nominally beyond the scope of available commercial codes, and is addressed in the published literature only in a limited sense. The dynamics of the system comprising the space station and the moving mobile transporter, mated to the orbiter or to the payload-carrying robotic arm, offers related challenges. A novel analytical approach is presented that can be used to study the dynamics behavior of such time-variant structural systems as the mobile transporter during space station operation and/or assembly. The approach developed herein is based on the formation of a linear transformation that expressses displacement compatibility at the time-variant interface domain of two flexible bodies. The methodology is readily applicable to large structural systems. The required inputs that characterize the structural system constitute readily available finite-element data. A model reduction scheme is developed wherein component modes of the parent linear-time-invariant problem are employed. Numerical results are provided.

I. Introduction

THE published theoretical literature in the domain of moving load problems does not generally address the relative motion of flexible bodies with multipoint contact. In previous work,[1–4] typical assumptions are made that restrict the applicability of the analysis. This paper presents a methodology that removes several restrictions and that is broader in scope. In the current analytical development the following is assumed.

1) The moving load is inertial (motion dependent).

2) A spatially discrete representation of the dynamics equations is used (finite element).

3) The structural system may be inertially free.

4) Both bodies may be flexible.

5) The relative nominal motion of the structures are prescribed. (The analysis easily lends itself to the elimination of this assumption.)

Available computer simulations[5–11] do not offer the listed generality. In particular, multibody codes such as DISCOS,[5] ADAMS,[6] or DADS[7] do not currently model flexible moving surface contact problems. Although DISCOS models flexibility in a general fashion, contiguous structures interact only via a set of well-defined stationary joints (telescopic joints are stationary as well).

The flexible body dynamics code NASTRAN can be used to analyze low-order structures involving a moving point-mass.[1,8] A Lagrange multiplier method is employed to produce a set of governing equations that possesses the morphology of a linear-time-invariant system and are thereby solvable within the computational infrastructure of NASTRAN. This method is potentially well suited to low-order problems.

The work presented in this paper is motivated by the dynamics problem posed by the space station (SS). Of interest is the operation of a vehicle [mobile transporter (MT)] that moves on two flexible rails and that carries payloads held by a flexible robotic arm. In essence, this problem involves the relative motion of two flexible bodies: 1) the SS-truss/rail structure and 2) the MT/arm/payload structure. Therefore, the generality of the presented approach is potentially required for modeling the dynamics of the described system.

The work presented herein is generic in nature and thereby not affected by the continual evolution of the SS program. The analytical development, together with the resulting computational algorithms, retains broad applicability. In addition, the techniques presented in this paper can be applied to railroad and other moving load problems.

This paper is organized as follows. The Introduction is followed by the system kinematics section, where the kinematics variables and the generic mathematical representation of the motion constraint are introduced. The third section develops and discusses the governing set of nonlinear time-invariant system dynamics equations. These equations are first developed in physical space. A model reduction approach is then devised for applications involving high-order structural systems. A qualitative discussion of the form of the dynamics equations is also presented. The fourth section addresses in detail the subject of motion constraint. This section presents a general method for prescribing the motion of one flexible body over another flexible body. Section V presents a numerical example and Sec. VI the conclusion.

Regarding notation, in the interest of readability, the functional dependencies of the variables are sometimes omitted when the context is unambiguous. Both visual clarity and consistency of notation were key considerations in notational matters.

II. System Kinematics

Figure 1a depicts the kinematics of a system comprising two flexible bodies. These two bodies are interchangeably referred to as the base body and the moving body, or body 1 and body 2, respectively. The base body can be either inertially free or inertially fixed, as required by the situation at hand. For example, for a pinned-pinned beam on which a mass is moving, the base body is inertially fixed. In cases involving space vehicles, the base body is inertially free. To allow for the relative motion of the two bodies along a track, the moving body is treated as being inertially free. It is assumed that finite element mass and stiffness matrices are available for each body and that those matrices are expressed relative to the same inertial frame.

The generalized coordinates are classified as follows. The vectors $\boldsymbol{q}_1$ and $\boldsymbol{q}_2$ are of dimensions n_1 and n_2, respectively, and denote the degrees of freedom (DOFs) that describe the absolute nodal displacement fields of body 1 and body 2. Subsets of those vectors are defined as q_{1i}, q_{1b}, q_{1c}, q_{2i}, q_{2b}, and q_{2c}, and are of dimension n_{1i}, n_{1b}, n_{1c}, n_{2i}, n_{2b}, and n_{2c}, respectively. The subscript i refers to the set of DOFs that are internal and will not experience interbody generalized constraint forces during the course of the bodies' relative motion. The subscript b refers to boundary DOFs/nodes or those that will experience generalized constraint forces during the course of the maneuver. Finally, the subscript c indicates constraint and refers to those DOFs that are instantaneously experiencing generalized

Received Feb. 8, 1995; revision received Dec. 1, 1995; accepted for publication Dec. 14, 1995.

*Associate Professor, Multidisciplinary Design Laboratory, Mechanical Engineering Department. Associate Fellow AIAA.

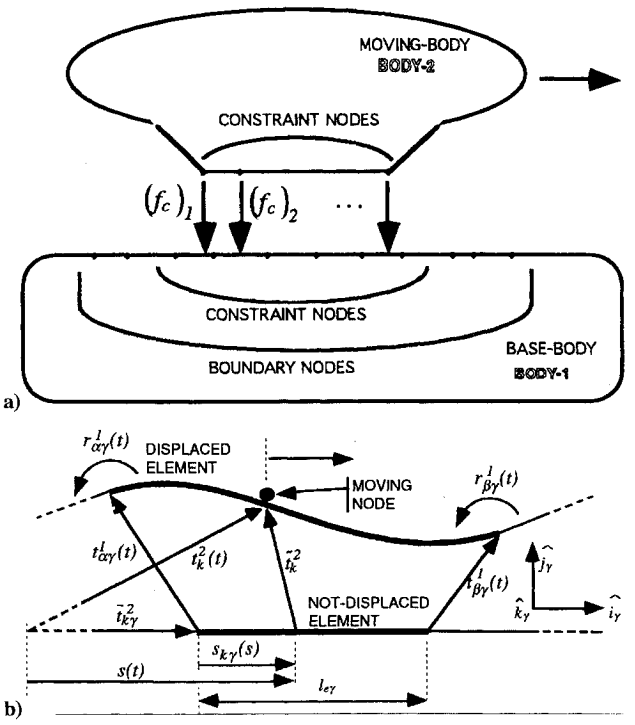

Fig. 1 Kinematics modeling: a) system kinematics and b) contact kinematics for generic element.

constraint forces. This latter set is time varying in body 1 and time invariant in body 2. From the preceding definitions and from the kinematics of the problem at hand (see Fig. 1a), it follows that the boundary and the constraint DOFs of body 2 are identical.

The set of constraint forces and torques is denoted by the n_c-dimensional vector $\boldsymbol{F}_c$, which comprises the constraint forces f_c and the constraint torques t_c. To be explicit, let $\boldsymbol{F}_c$ represent the forces and torques that the contact-nodes on body 2 apply to body 1. Observe that since $q_{2b} = q_{2c}$, then $n_{2b} = n_{2c} = n_c$, and that $n_{1i} + n_{1b} = n_1$ and $n_{2i} + n_{2b} = n_2$.

The rigid-body position of body 2 relative to body 1 is prescribed by a coordinate denoted by $s(t)$. As will be seen, $s(t)$ partially prescribes the motion of a generic contact node of body 2.

In a generic fashion, the motion constraint is assumed governed by the relation

$$\boldsymbol{q}_{2b}[s(t), t] = G[s(t)]\boldsymbol{q}_{1b}(t) + \boldsymbol{p}[s(t)] \tag{1}$$

where $G[s(t)]$ is an appropriately dimensioned mapping matrix and $p[s(t)]$ is that component of q_{2b} that does not depend on q_{1b} (which is prescribed). As expected, $p[s(t)]$ depends on $s(t)$. A great deal of care is required in the detailed development of Eq. (1). A comprehensive discussion of this development is presented in Sec. IV, Motion Constraint.

In accordance with these definitions, the physical coordinates are written as

$$\boldsymbol{q}_1(t) = \begin{Bmatrix} \boldsymbol{q}_{1i}(t) \\ \boldsymbol{q}_{1b}(t) \end{Bmatrix}, \qquad \boldsymbol{q}_2[s(t), t] = \begin{Bmatrix} \boldsymbol{q}_{2i}(t) \\ \boldsymbol{q}_{2b}[s(t), t] \end{Bmatrix} \tag{2}$$

Using these kinematics, the system dynamics equations are developed.

III. System Dynamics Equations

Section III develops and discusses the system dynamics equations. This development is performed in three steps. First, the governing equation of motion for each body is independently formed without enforcing interbody displacement compatibility. This involves developing 1) the base-body equation and 2) the moving-body equation, followed by 3) the concatenation of these equations into a single system matrix equation. Second, a linear transformation matrix is developed that, when employed, has the dual consequence of enforcing displacement compatibility and of reducing the order of the system. Third, the system governing equations of motion is obtained with the aid of the derived transformation. These three steps are carried out in the sequel.

A. System Equations Without Displacement Compatibility

1. Base-Body Equation

The base-body's equation of motion is expressed as

$$M_1 \frac{\mathrm{d}^2}{\mathrm{d}t^2}\boldsymbol{q}_1 + D_1 \frac{\mathrm{d}}{\mathrm{d}t}\boldsymbol{q}_1 + K_1\boldsymbol{q}_1 = \boldsymbol{F}_{1e} + E_1\boldsymbol{F}_c \tag{3}$$

where M_1, D_1, and K_1 are mass, damping, and stiffness matrices respectively, of dimension $n_1 \times n_1$. The vector $\boldsymbol{F}_{1e}$ denotes externally applied generalized forces. The quantity E_1 is a time-varying influence coefficient matrix that depends on the instantaneous relative spatial location of the interface of the two bodies. To fix ideas, the variables of Eq. (3) and their dimensions are explicitly expressed as

$$\boldsymbol{q}_1 = \begin{Bmatrix} \boldsymbol{q}_{1i}^{n_{1i}\times 1} \\ \boldsymbol{q}_{1b}^{n_{1b}\times 1} \end{Bmatrix}^{n_1\times 1} \tag{4}$$

$$\boldsymbol{F}_{1e} = \begin{Bmatrix} \boldsymbol{f}_{1e}^{n_{1i}\times 1} \\ \boldsymbol{0}^{n_{1b}\times 1} \end{Bmatrix}^{n_1\times 1}, \qquad E_1 = \begin{Bmatrix} 0 \\ E_{1b}^{n_{1b}\times n_c} \end{Bmatrix}^{n_1\times n_c} \tag{5}$$

The matrix E_1 can be evaluated in various ways. One approach is to express the virtual work associated with the generalized constraint forces in two different forms and to compare the two results. The first expression is obtained by considering the virtual work performed by the constraint force on body 1 as

$$\delta W_1(t) = (E_{1b}\boldsymbol{F}_c)^T \delta\boldsymbol{q}_{1b}(t) \tag{6}$$

In the second expression, the virtual work performed by the constraint force on body 2 is written as

$$\begin{aligned} \delta W_2(t) &= -\boldsymbol{F}_c^T \delta\boldsymbol{q}_{2b}[s(t), t] \qquad \text{[from Eq. (1)]} \\ &= -\boldsymbol{F}_c^T \delta[G\boldsymbol{q}_{1b}(t)] \\ &= -\left(G^T\boldsymbol{F}_c\right)^T \delta\boldsymbol{q}_{1b}(t) \end{aligned} \tag{7}$$

Since the sum of $\delta W_1(t)$ and $\delta W_2(t)$ must vanish, Eqs. (6) and (7) lead to

$$G^T = E_{1b} \tag{8}$$

2. Moving-Body Equation

The moving-body's governing equation is similarly expressed as

$$M_2 \frac{\mathrm{d}^2}{\mathrm{d}t^2}\boldsymbol{q}_2 + D_2 \frac{\mathrm{d}}{\mathrm{d}t}\boldsymbol{q}_2 + K_2\boldsymbol{q}_2 = \boldsymbol{F}_{2e} + E_2\boldsymbol{F}_c \tag{9}$$

where M_2, D_2, and K_2 are mass, damping, and stiffness matrices, respectively, of dimension $n_2 \times n_2$. Also, $\boldsymbol{F}_{2e}$ represents the externally applied generalized forces and E_2 is a constant influence coefficient matrix that prescribes the location of the constraint forces. The analogs of Eqs. (4) and (5) take the form

$$\boldsymbol{q}_2 = \begin{Bmatrix} \boldsymbol{q}_{2i}^{n_{2i}\times 1} \\ \boldsymbol{q}_{2b}^{n_{2b}\times 1} \end{Bmatrix}^{n_2\times 1} \tag{10}$$

$$F_{2e} = \begin{Bmatrix} \boldsymbol{f}_{2e}^{n_{2i}\times 1} \\ \boldsymbol{0}^{n_{2b}\times 1} \end{Bmatrix}^{n_2\times 1}, \qquad E_2 = \begin{Bmatrix} 0 \\ -I^{n_c\times n_c} \end{Bmatrix}^{n_2\times n_c} \tag{11}$$

The base- and moving-body equations can conveniently be expressed as a single matrix equation, as is done in the sequel.

3. System Equation Without Displacement Compatibility

For the purpose of facilitating the system equation development, Eqs. (3) and (9) are concatenated into a single equation as

$$\bar{M}\frac{\mathrm{d}^2}{\mathrm{d}t^2}\bar{q} + \bar{D}\frac{\mathrm{d}}{\mathrm{d}t}\bar{q} + \bar{K}\bar{q} = \bar{F}_e + \bar{E}F_c \tag{12}$$

where

$$\bar{q} = \begin{Bmatrix} q_1 \\ q_2 \end{Bmatrix}, \qquad \bar{F}_e = \begin{Bmatrix} F_{1e} \\ F_{2e} \end{Bmatrix}, \qquad \bar{E} = \begin{bmatrix} E_1 \\ E_2 \end{bmatrix} \tag{13}$$

$$\bar{M} = \begin{bmatrix} M_1 & 0 \\ 0 & M_2 \end{bmatrix}, \qquad \bar{D} = \begin{bmatrix} D_1 & 0 \\ 0 & D_2 \end{bmatrix}$$

$$\bar{K} = \begin{bmatrix} K_1 & 0 \\ 0 & K_2 \end{bmatrix} \tag{14}$$

Note that both Eqs. (1) and (12) are required to completely define the system dynamics. The system contains $n_1 + n_2 - n_c$ independent dynamic DOFs: Eq. (12) contains $n_1 + n_2$ scalar equations, and Eq. (1) contains n_c constraints.

B. Transformation Matrix for Displacement Compatibility and Model Reduction

The system equation, Eq. (12), does not yet reflect displacement compatibility at the interface of the two bodies. A system displacement-compatibility equation must be developed for that purpose. In addition, a model reduction scheme is required for the purpose of numerical simulation of high-order systems.

To do so, a transformation/mapping matrix is formed in three steps: 1) Develop a displacement-compatibility relation for the full-order system. 2) Develop a model reduction approach. 3) Develop the mapping from the unconstrained space [Eq. (13)] to the constrained and reduced-order system space.

1. Displacement Compatibility for Full-Order System

Using Eqs. (1), (2), and (13), the displacement-compatibility coordinate transformation is expressed as

$$\bar{q}[s(t), t] = \bar{T}[s(t)]q[s(t), t] + \bar{p}[s(t)] \tag{15}$$

where

$$q = \begin{Bmatrix} q_{1i} \\ q_{1b} \\ q_{2i} \end{Bmatrix}; \qquad \bar{p}[s(t)] = \begin{Bmatrix} 0 \\ 0 \\ 0 \\ p[s(t)] \end{Bmatrix} \tag{16}$$

and

$$\bar{T}[s(t)] = \begin{bmatrix} I & 0 & 0 \\ 0 & I & 0 \\ 0 & 0 & I \\ 0 & G[s(t)] & 0 \end{bmatrix} \tag{17}$$

Two observations are made: 1) $\bar{T}[s(t)]$ is of rank $n_1 + n_2 - n_c$, and 2) this transformation spans the orthogonal complement of the generalized constraint force space. The matrix $\bar{E}$ lies in the null space of $\bar{T}^T$, that is,

$$\bar{T}^T[s(t)]\bar{E}[s(t)] = 0 \tag{18}$$

Accordingly, the set of constrained governing equations can be obtained by substituting Eq. (15) into Eq. (12), followed by premultiplication by $\bar{T}^T$. Before performing this manipulation, model reduction is addressed.

2. Model Reduction Approach

A model reduction approach, for the two-body dynamical system previously described, is now developed. The intent is to produce a coordinate transformation that will result in a set of low-order equations that faithfully captures the system dynamics. In considering the possible model reduction options, one immediately observes that the standard modal model reduction for each body is not necessarily the best choice. When the number of displacement constraints (n_{2c}) is large, it is impossible to satisfy displacement compatibility satisfactorily without including an unduly large number of modes. This is because one cannot prescribe n_{2c} displacement constraint conditions using a lesser number of generalized coordinates for body 2. Fortunately, one can exploit the freedom in the choice of modes to simplify the form of the ensuing quantities.

The approach employed is characterized by modal model reduction for body 1, and model reduction for body 2 where the boundary generalized coordinates (q_{2b}) are maintained. This approach is implemented as follows.

Step 1: Perform a standard modal decomposition for body 1, as

$$q_1 \equiv \begin{Bmatrix} q_{1i} \\ q_{1b} \end{Bmatrix} = \phi_1\eta_1, \qquad \phi_1 = \begin{bmatrix} \phi_{1i} \\ \phi_{1b} \end{bmatrix} \tag{19}$$

where the modes are normalized as

$$\phi_1^T M_1\phi_1 = I, \qquad \phi_1^T K_1\phi_1 = \Lambda_1 \tag{20}$$

and where the variables take on standard definitions.

Damping for body 1 is assumed to take the typical form

$$\phi_1^T D_1\phi_1 = 2\zeta_1\sqrt{\Lambda_1} \tag{21}$$

where

$$\zeta_1 = \mathrm{diag}\{\zeta_{11} \quad \zeta_{12} \quad \cdots\} \tag{22}$$

comprises modal damping ratios.

Step 2: Perform model reduction for body 2, where the constraint node coordinates (q_{2b}) are retained in physical space. Note that this does not adversely impact the efficiency of model reduction, since the number of constraint nodes in body 2 does not impact the order of the system equation [as will be seen in Eqs. (34), (38), and (39)].

This model reduction takes the form

$$q_2 = \begin{Bmatrix} q_{2i} \\ q_{2b} \end{Bmatrix} \equiv \phi_2 \begin{Bmatrix} \eta_{2i} \\ q_{2b} \end{Bmatrix}, \qquad \phi_2 = \begin{bmatrix} \phi_{2ii} & \phi_{2ib} \\ 0 & I \end{bmatrix} \tag{23}$$

where the partitioning is self-explanatory but the partitions are as yet undefined.

Several well-known methods are available for choosing the two upper partitions of the transformation matrix ϕ_2 in Eq. (23). The approach employed here borrows some aspects of the work presented in Ref. 12 by letting

$$\phi_{2ii}^T M_{2ii}\phi_{2ii} = I, \qquad \phi_{2ii}^T K_{2ii}\phi_{2ii} = \Lambda_2 \tag{24}$$

and

$$\phi_{2ib} = -(K_{2ii})^{-1}K_{2ib} \tag{25}$$

where

$$M_k \equiv \begin{bmatrix} M_{kii} & M_{kib} \\ M_{kbi} & M_{kbb} \end{bmatrix} \qquad (k = 1, 2) \tag{26}$$

$$K_k \equiv \begin{bmatrix} K_{kii} & K_{kib} \\ K_{kbi} & K_{kbb} \end{bmatrix} \qquad (k = 1, 2) \tag{27}$$

where the subscripts i and b pertain to internal and boundary DOFs, respectively.

The specific form of Eq. (25) is responsible for the convenient cancellation of the off-diagonal partition of a reduced-order stiffness matrix. [This is seen later in Eq. (54).]

To develop an acceptable representation of the viscoelastic damping of body 2, it is appropriate to observe the following:

a) The internal and boundary nodes of body 1 are already damped [see Eq. (21)].

b) The boundary nodes of body 2 are also already damped since they depend on those of body 1, which are damped.

c) Only the internal DOFs of body 2 still need damping.

The damping representation is then judiciously chosen to be of the form

$$\phi_2^T D_2 \phi_2 = \begin{bmatrix} 2\zeta_2\sqrt{\Lambda_2} & 0 \\ 0 & 0 \end{bmatrix} \tag{28}$$

where

$$\zeta_2 = \text{diag}\{\zeta_{21} \quad \zeta_{22} \quad \cdots\} \tag{29}$$

comprises modal damping ratios. Observe that, as planned, damping is provided only for the internal DOFs. In addition, this representation of the damping [Eq. (28)] is responsible for an appealing form of the resulting system damping matrix [as will be seen in Eq. (64)].

Step 3: Combine Eqs. (1), (19), and (23) to obtain the modal transformation

$$q = \begin{bmatrix} q_{1i} \\ q_{1b} \\ q_{2i} \end{bmatrix} = \phi[s(t)]\eta + \tilde{p}[s(t)] \tag{30}$$

where

$$\phi[s(t)] = \begin{bmatrix} \phi_{1i} & 0 \\ \phi_{1b} & 0 \\ \phi_{2ib} G \phi_{1b} & \phi_{2ii} \end{bmatrix} \tag{31}$$

$$\eta(t) = \begin{Bmatrix} \eta_1 \\ \eta_{2i} \end{Bmatrix}, \qquad \tilde{p}[s(t)] = \begin{Bmatrix} 0 \\ 0 \\ \phi_{2ib} p(s) \end{Bmatrix} \tag{32}$$

It is critical to observe that the resulting modal matrix ϕ is not constant because it involves G. Accordingly, modal substitution in the conventional sense is not applicable. Special care is in order.

3. Coordinate Transformation from Unconstrained System to Reduced-Order/Constrained System

The coordinate transformation that reflects both displacement compatibility and model reduction is obtained by combining Eqs. (15) and (30). This leads to a transformation of the form

$$\bar{q}[s(t), t] = T[s(t)]\eta(t) + \tilde{\phi} p[s(t)] \tag{33}$$

where

$$T[s(t)] = \bar{T}[s(t)]\phi[s(t)], \qquad \tilde{\phi} = \begin{Bmatrix} 0 \\ 0 \\ \phi_{2ib} \\ I \end{Bmatrix} \tag{34}$$

The preceding coordinate transformation is employed for obtaining the constrained and reduced-order set of equations. For later use, the first and second derivatives of Eq. (33) are evaluated as

$$\frac{\mathrm{d}}{\mathrm{d}t}\bar{q}[s(t), t] = \dot{s} T_s \eta + T\dot{\eta} + \dot{s}\tilde{\phi} p_s \tag{35}$$

$$\frac{\mathrm{d}^2}{\mathrm{d}t^2}\bar{q}[s(t), t] = \ddot{s} T_s \eta + 2\dot{s} T_s \dot{\eta} + T\ddot{\eta} + \dot{s}^2(T_{ss}\eta + \tilde{\phi} p_{ss}) + \ddot{s}\tilde{\phi} p_s \tag{36}$$

where, for convenience, the notations

$$\frac{\partial(\,)}{\partial s} \equiv (\,)_s; \qquad \frac{\partial(\,)}{\partial t} \equiv \dot{(\,)} \tag{37}$$

are invoked. Note that the first and second derivatives of the trajectory with respect to the coordinate s must exist [see p_{ss} in Eq. (36)]. As a consequence, the trajectory should not involve the boundaries of any finite elements that do not satisfy the condition. Special care must be taken when modeling the motion of a cart on a truss structure. Nonbending axial-strain elements would not be acceptable.

C. System Equations with Displacement Compatibility and Model Reduction

The governing equation is obtained by substituting Eqs. (33), (35), and (36) into Eq. (12), followed by premultiplication by T^T and use of Eq. (18). The resulting set of equations is then obtained in the form

$$M_0(s)\ddot{\eta}(t) = F_e(s, t) - F_m(s, \dot{s}, \ddot{s}, \eta, \dot{\eta}) \tag{38}$$

where

$$M_0 = T^T \bar{M} T \tag{39}$$

$$F_e(s, t) = T^T(s)\bar{F}_e(t) \tag{40}$$

and

$$F_m(s, \dot{s}, \ddot{s}, \eta, \dot{\eta}) = F_0(s, \eta, \dot{\eta}) + \dot{s}F_\alpha(s, \eta, \dot{\eta}) + \ddot{s}F_\beta(s, \eta) + \dot{s}^2 F_\gamma(s, \eta) \tag{41}$$

The various force components have the form

$$F_0(s, \eta, \dot{\eta}) = D_0\dot{\eta} + K_0(s)\eta + \tilde{K}_0(s)p(s) \tag{42}$$

$$F_\alpha(s, \eta, \dot{\eta}) = 2D_\alpha(s)\dot{\eta} + K_\alpha(s)\eta + \tilde{K}_\alpha(s)p_s(s) \tag{43}$$

$$F_\beta(s, \eta) = K_\beta(s)\eta + \tilde{K}_\beta(s)p_s(s) \tag{44}$$

$$F_\gamma(s, \eta) = K_\gamma(s)\eta + \tilde{K}_\gamma(s)p_{ss}(s) \tag{45}$$

Equation (42) shows the force terms that are not dependent on the relative motion of the two bodies along the track. Equations (43) and (44) display those terms that are dependent on the relative velocity $\dot{s}$ and on the relative acceleration $\ddot{s}$, respectively. Equation (45) accounts for the terms that are proportional to the square of the relative velocity.

The constituent components of Eqs. (42–45) are expressed more explicitly in three categories: the effective-damping terms that are proportional to $\dot{\eta}$,

$$D_0 = T^T \bar{D} T, \qquad D_\alpha = T^T \bar{M} T_s \tag{46}$$

the effective-stiffness terms that are proportional to η,

$$K_0 = T^T \bar{K} T, \qquad K_\alpha = T^T \bar{D} T_s \tag{47}$$

$$K_\beta = T^T \bar{M} T_s, \qquad K_\gamma = T^T \bar{M} T_{ss} \tag{48}$$

and the effective-stiffness terms that are dependent on the trajectory,

$$\tilde{K}_0 = T^T \bar{K}\tilde{\phi}, \qquad \tilde{K}_\alpha = T^T \bar{D}\tilde{\phi} \tag{49}$$

$$\tilde{K}_\beta = \tilde{K}_\gamma = T^T \bar{M}\tilde{\phi} \tag{50}$$

It is desirable to decipher the physical meaning of the various terms depicted in Eqs. (46–50). In addition to gaining physical insight into the problem, this effort will also serve the purpose of computational efficiency. When it is known that a certain physical effect does not apply to the situation at hand, one can simply bypass that part of the computation.

For example, two terms that would identically vanish (and should not be computed) in the case of the mobile transporter are briefly discussed:

1) The last term of Eq. (42) represents a static generalized force that is produced by a mismatch in the position of the two contact points in their undeformed states.

2) The last term of Eq. (45) depicts an inertial force that is the result of the curvature of the trajectory in its undeformed states.

1. Explicit Representation

Equations (39–50) provide a clear top-level view of the constituent components of the governing equation [Eq. (38)]. Additional insight is gained by expressing Eqs. (39) and (46–50) in a more detailed form.

Combining appropriate equations leads to

$$M_0 = \begin{bmatrix} I + \phi_{2c}^T M_2 \phi_{2c} & \phi_{2c}^T M_2 \phi_{2n} \\ \phi_{2n}^T M_2 \phi_{2c} & I \end{bmatrix} \tag{51}$$

$$D_0 = \begin{bmatrix} 2\zeta_1\sqrt{\Lambda_1} & 0 \\ 0 & 2\zeta_2\sqrt{\Lambda_2} \end{bmatrix} \tag{52}$$

$$D_\alpha = \begin{bmatrix} \phi_{2c}^T M_2 (\phi_{2c})_s & 0 \\ \phi_{2n}^T M_2 (\phi_{2c})_s & 0 \end{bmatrix} \tag{53}$$

$$K_0 = \begin{bmatrix} \Lambda_1 + \phi_{2c}^T K_2 \phi_{2c} & 0 \\ 0 & \Lambda_2 \end{bmatrix} \tag{54}$$

$$K_\alpha = \begin{bmatrix} 0 & 0 \\ 0 & 0 \end{bmatrix} \tag{55}$$

$$K_\beta = \begin{bmatrix} \phi_{2c}^T M_2 (\phi_{2c})_s & 0 \\ \phi_{2n}^T M_2 (\phi_{2c})_s & 0 \end{bmatrix} \tag{56}$$

$$K_\gamma = \begin{bmatrix} \phi_{2c}^T M_2 (\phi_{2c})_{ss} & 0 \\ \phi_{2n}^T M_2 (\phi_{2c})_{ss} & 0 \end{bmatrix} \tag{57}$$

$$\tilde{K}_0 = \begin{bmatrix} \phi_{2c}^T K_2 \tilde{\phi}_2 \\ \phi_{2n}^T K_2 \tilde{\phi}_2 \end{bmatrix} \tag{58}$$

$$\tilde{K}_\alpha = \begin{bmatrix} \phi_{2c}^T D_2 \tilde{\phi}_2 \\ \phi_{2n}^T D_2 \tilde{\phi}_2 \end{bmatrix} = \begin{bmatrix} 0 \\ 0 \end{bmatrix} \tag{59}$$

$$\tilde{K}_\beta = \tilde{K}_\gamma = \begin{bmatrix} \phi_{2c}^T M_2 \tilde{\phi}_2 \\ \phi_{2n}^T M_2 \tilde{\phi}_2 \end{bmatrix} \tag{60}$$

where

$$\phi_{2c} = \begin{bmatrix} \phi_{2ib} G \phi_{1b} \\ G\phi_{1b} \end{bmatrix}, \quad \phi_{2n} = \begin{bmatrix} \phi_{2ii} \\ 0 \end{bmatrix}, \quad \tilde{\phi}_2 = \begin{bmatrix} \phi_{2ib} \\ I \end{bmatrix} \tag{61}$$

Note that the lower-right-hand block of Eq. (52) is obtained with the aid of Eqs. (23) and (28). This completes the development of the governing equations in modal coordinates.

2. Qualitative Discussion of Dynamics Equations

The following comments provide a qualitative discussion of the dynamics equations just developed. To facilitate the discussion, Eq. (38) is expressed more explicitly as

$$M_0\ddot{\eta} + [D_0 + 2D_\alpha \dot{s}]\dot{\eta} + \left[K_0 + K_\beta \ddot{s} + K_\gamma \dot{s}^2\right]\eta$$

$$= F_e - \tilde{K}_0 p - \tilde{K}_\beta p_s \ddot{s} - \tilde{K}_\gamma p_{ss} \dot{s}^2 \tag{62}$$

which leads to the following observations:

a) The matrices M_0, D_0, and K_0 represent the matrices of the linear-time-invariant system that result when the two bodies are stationary relative to each other.

b) The matrix D_α, multiplied by $\dot{s}$, represents an effective motion-induced damping component.

c) In a similar vein, the matrices K_β and K_γ represent motion-induced stiffnesses. In the case of constant or slow relative speed of the two bodies, K_β or K_γ would become negligible, respectively. Observe also that K_β is related to interface-deformation slope [Eq. (56)], whereas K_γ relates to interface-deformation curvature [Eq. (57)].

d) The matrices $\tilde{K}_0$, $\tilde{K}_\beta$, and $\tilde{K}_\gamma$ contribute to effective forcing terms that are caused by the contact-interface shapes. $\tilde{K}_0$ is caused by interface mismatch in the undeformed state, whereas $\tilde{K}_\beta (= \tilde{K}_\gamma)$ is related to interface curvature. In the case where the interface consists of straight rails, all of these terms vanish.

These observations provide insight into the equations governing this class of moving load problems. Interestingly, many of these terms and many of these observations find their analogs in the simpler cases of Refs. 1–4.

The next section develops the interface kinematic constraint equations that are used to develop the system equations.

IV. Motion Constraint

A. Contact Modeling Issues

Section IV explicitly develops the mathematical expression that prescribes the contact between the two bodies. Recall that both bodies may be flexible and move about each other. This kinematic constraint is represented by Eq. (1) and is repeated here for convenience as

$$q_{2b}[s(t), t] = G[s(t)]q_{1b}(t) + p[s(t)] \tag{63}$$

Equation (63) depicts the dependence of the boundary nodes of body 2 (q_{2b}) on those of body 1 (q_{1b}) and on the coordinate s. This nodal dependence forms the essence of the contact modeling. Observe that, in tandem with the discrete modeling approach employed in this analysis, the displacement field of the contact domain is expressed with the aid of discrete variables. The set of generalized coordinates representing the translational and rotational displacements at a finite number of points is employed (q_{1b} and q_{2b}).

The corresponding spatially continuous displacement field of the contact interface is obtained by employing interpolation functions. Although any twice-differentiable set of functions could be used as an approximation, the most appropriate candidate set is that which is employed in the finite element analysis of the structure.

The coordinate s is considered a scalar throughout this analysis. This is appropriate in the case when the relative motion of a structure is prescribed along a track (with no additional relative rigid-body motion). In more general cases, a prescribed set of independent coordinates would be employed, and the basic philosophy of the analysis presented herein would remain unchanged.

For the purpose of simplicity of presentation, and with the case of the SSMT in mind, the motion of body 2 relative to body 1 is assumed to take place along a rectilinear track.

B. Contact Kinematics

The contact kinematics are modeled in two steps by considering the constituent components of the system in their primordial state. For the purpose of kinematics modeling, two primordial entities are considered: a generic boundary node of body 2 and the generic element of body 1 on which the boundary node moves. Step 1 is to analyze and mathematically express that node's motion as it moves across a generic constituent element of the finite element model of body 1 [see Eqs. (64) and (65)]. Step 2 is to analyze the relative motion of the contact interfaces in terms of the motion of their constituent nodes [see Eq. (66)].

Figure 1b depicts the kinematics of the generic kth node of body 2 while that node moves over the γth element of body 1. The γth element is assumed bounded by two nodes, α and β, whose respective translations are denoted by the vectors $t_\alpha^1(t)$ and $t_\beta^1(t)$ and rotations by $r_\alpha^1(t)$ and $r_\beta^1(t)$. The preceding four vectors are expressed in a global inertial frame. A local γ-element frame is represented by the dextral triad of unit vectors $\{\hat{i}_\gamma, \hat{j}_\gamma, \hat{k}_\gamma\}$. The vector $t_k^2(t)$ represents the absolute displacement of the generic node k of body 2.

The constituent components of the vector $t_k^2(t)$ are 1) the scalar coordinate $\bar{t}_{k\gamma}^2$, which locates the position of node α (of the γ element) relative to node k before displacement of either node; 2) the scalar coordinate $s_{k\gamma}(s)$, which denotes the prescribed motion of node k ($s_{k\gamma} = s - \bar{t}_{k\gamma}^2$); and 3) the vector $\bar{t}_k^2$, which denotes the remaining component of the vector t_k^2. (The latter component, $\bar{t}_k^2$, will be represented by means of interpolation functions.)

Note that all of the quantities with the double subscript $k\gamma$ are defined only when node k is moving on element γ.

For notational convenience, let the six-dimensional nodal displacement at the kth generic node be represented by

$$u_k^{p(6\times 1)} = \begin{Bmatrix} t_k^p \\ r_k^p \end{Bmatrix}, \qquad \{p = 1, 2\} \tag{64}$$

where t_k^p and r_k^p denote the translation and rotation of the kth node of the pth body, respectively.

In the sequel, displacement compatibility is expressed for a discrete finite set of nodal translational displacements. In some cases, the physical situation might require expressing compatibility with the vector $\boldsymbol{u}_k^p$, rather than simply with $\boldsymbol{t}_k^p$. That extension is conceptually straightforward (and would not be required in the case of the MT, where translational compatibility is sufficient).

The next step in forming the constraint equation is to express the displacement of a generic node of body 2, $\boldsymbol{t}_k^2$, in terms of the generalized displacements of two neighboring nodes, $\boldsymbol{u}_\alpha^1$ and $\boldsymbol{u}_\beta^1$, via interpolation. (In the case of, say, plate elements, more than two neighboring nodes would be used in the interpolation. That extension, too, is straightforward.)

In terms of the variables defined above, the absolute displacement of node k of body 2 is written as

$$\boldsymbol{t}_k^2 = \tilde{\boldsymbol{p}} + \tilde{\boldsymbol{t}}_k^2, \qquad \tilde{\boldsymbol{p}} = C^\gamma \begin{Bmatrix} s \\ 0 \\ 0 \end{Bmatrix} \tag{65}$$

where C^γ transforms a generic vector from the local γ-element frame to the global frame. Note that, when the vehicle trajectory is a straight line, it is beneficial to let one of the axes of the global frame be parallel to the trajectory.

Next, displacement compatibility is invoked by expressing the vector $\tilde{\boldsymbol{t}}_k^2$ in terms of the neighboring generalized displacement vectors of body 1 as

$$\tilde{\boldsymbol{t}}_k^2 = \tilde{T}_{\alpha k}(\xi_k)\boldsymbol{u}_\alpha^1(t) + \tilde{T}_{\beta k}(\xi_k)\boldsymbol{u}_\beta^1(t) \tag{66}$$

where

$$\xi_k(\gamma, s) = \frac{s_{k\gamma}(s)}{l_{e\gamma}}, \qquad s_{k\gamma} = s - \tilde{t}_{k\gamma}^2 \tag{67}$$

$$\tilde{T}_{\alpha k}(\xi_k) = C^\gamma T_{\alpha k}(\xi_k)\bar{C}^{\gamma T} \tag{68}$$

$$\tilde{T}_{\beta k}(\xi_k) = C^\gamma T_{\beta k}(\xi_k)\bar{C}^{\gamma T} \tag{69}$$

with

$$\bar{C}^\gamma = \begin{bmatrix} C^\gamma & 0 \\ 0 & C^\gamma \end{bmatrix} \tag{70}$$

The interpolation matrices are

$$T_{\alpha k}(\zeta_k) = \begin{bmatrix} T_{\alpha k}^l & 0 & 0 & 0 & 0 & 0 \\ 0 & T_{\alpha k}^b & 0 & 0 & 0 & T_{\alpha k}^r \\ 0 & 0 & T_{\alpha k}^b & T_{\alpha k}^r & 0 & 0 \end{bmatrix} \tag{71}$$

$$T_{\beta k}(\zeta_k) = \begin{bmatrix} T_{\beta k}^l & 0 & 0 & 0 & 0 & 0 \\ 0 & T_{\beta k}^b & 0 & 0 & 0 & T_{\beta k}^r \\ 0 & 0 & T_{\beta k}^b & T_{\beta k}^r & 0 & 0 \end{bmatrix} \tag{72}$$

where the superscripts l, b, and r pertain to longitudinal, bending, and rotational DOFs, respectively. The value of the subscript γ changes as the motion of body 2 along the rail progresses (with prior knowledge of the base structure's geometry and of the finite element description).

The transformation entries [see Eqs. (71) and (72)] contain linear interpolation functions for longitudinal deformation, whereas cubic shape functions are assumed for bending. These assumptions are consistent with those of beam elements. It is noted that the methods developed in this paper are not limited to the preceding assumptions, which are invoked here for simplicity of presentation and with the case of the space station mobile transporter in mind.

Explicit expressions for the interpolation functions are

$$T_{\alpha k}^l = 1 - \xi_k, \qquad T_{\beta k}^l = \xi_k \tag{73}$$

$$T_{\alpha k}^b = 1 - 3\xi_k^2 + 2\xi_k^3, \qquad T_{\beta k}^b = 3\xi_k^2 - 2\xi_k^3 \tag{74}$$

$$T_{\alpha k}^r = \left(\xi_k - 2\xi_k^2 + \xi_k^3\right)l_e, \qquad T_{\beta k}^r = \left(-\xi_k^2 + \xi_k^3\right)l_e \tag{75}$$

With the availability of Eqs. (65) and (66), the quantities $G[s(t)]$ and $\boldsymbol{p}[s(t)]$ of the constraint equation [Eq. (63)] take the form

$$G[s(t)] = \begin{bmatrix} \tilde{T}_{\alpha 1} & \tilde{T}_{\beta 1} & 0 & 0 & 0 & 0 \\ 0 & 0 & \tilde{T}_{\alpha 2} & \tilde{T}_{\beta 2} & 0 & 0 \\ 0 & 0 & 0 & 0 & \vdots & \vdots \end{bmatrix} \tilde{T} \tag{76}$$

where $\tilde{T}$ is a selection matrix defined by the relation

$$\{u_{\alpha 1} \quad u_{\beta 1} \quad u_{\alpha 2} \quad u_{\beta 2} \quad \cdots\}^T \equiv \tilde{T}\boldsymbol{q}_{1b} \tag{77}$$

and [see Eq. (65)]

$$\boldsymbol{p}[s(t)] = \{\tilde{\boldsymbol{p}} \quad \tilde{\boldsymbol{p}} \quad \cdots\}^T \tag{78}$$

Observe that $s_{k\gamma}$ typically takes on values ranging from zero to $l_{e\gamma}$, as the kth node moves over the γth element of body 1. As the kth node moves to the next element, $s_{k\gamma}$ discontinuously vanishes. Fortunately, the derivative of $s_{k\gamma}$ is not explicitly required, only that of $\tilde{\boldsymbol{t}}_k^2$ is [see Eq. (66)]. By careful thinking, it is possible to observe that the required partial derivatives relative to s do exist, if one is willing to use the values of the limits. This liberty is warranted, as this artificial situation was created not by the physical problem at hand but, rather, by the mathematical formalism employed.

This completes the development of the constraint equations, which are formally used in the dynamics equations development [see Eq. (1)].

V. Numerical Example

To illustrate the application of the methodology presented in this paper, this section provides numerical results for the case of a pinned-pinned beam and of a planar space truss. These examples were chosen to accomplish specific objectives. The beam example degenerates into a dynamical system that is analyzed in previously published work,[1] which allows for comparison of results. The truss example, too, lends itself to comparison with previously published results. Reference 13 analyzes a planar space beam that is subjected to the same vehicle forces. In light of the expected beamlike behavior of the chosen space truss, the numerical results (dynamics behavior) of the two systems should accordingly be similar.

In the sequel, the two examples are described. This description is followed by a nondimentionalization of the pertaining kinematics and dynamics variables, which leads to ease of interpretation of the results. Simulation results are then presented and compared with previously published work.

A. Physical System Examples

Figure 2a depicts a simply supported beam, which is modeled as a set of beam-elements (example 1). Figure 2b describes a free-free planar truss, on which a point mass travels (example 2). Whether the structure is inertially free or fixed, only the lateral motion is reported herein.

In Fig. 2a, a vehicle that has two wheels is assumed to travel on the structure at constant speed. The wheels are separated by a distance b, and $s(t)$ prescribes the motion of the vehicle along the

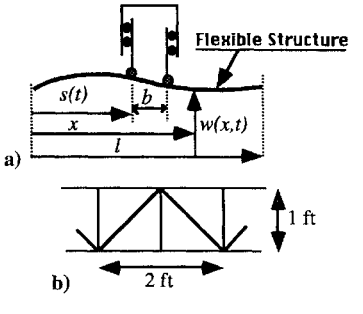

Fig. 2 Structure examples: a) two-wheel vehicle on simply supported beam, example 1, and b) planar free-free space-truss, example 2.

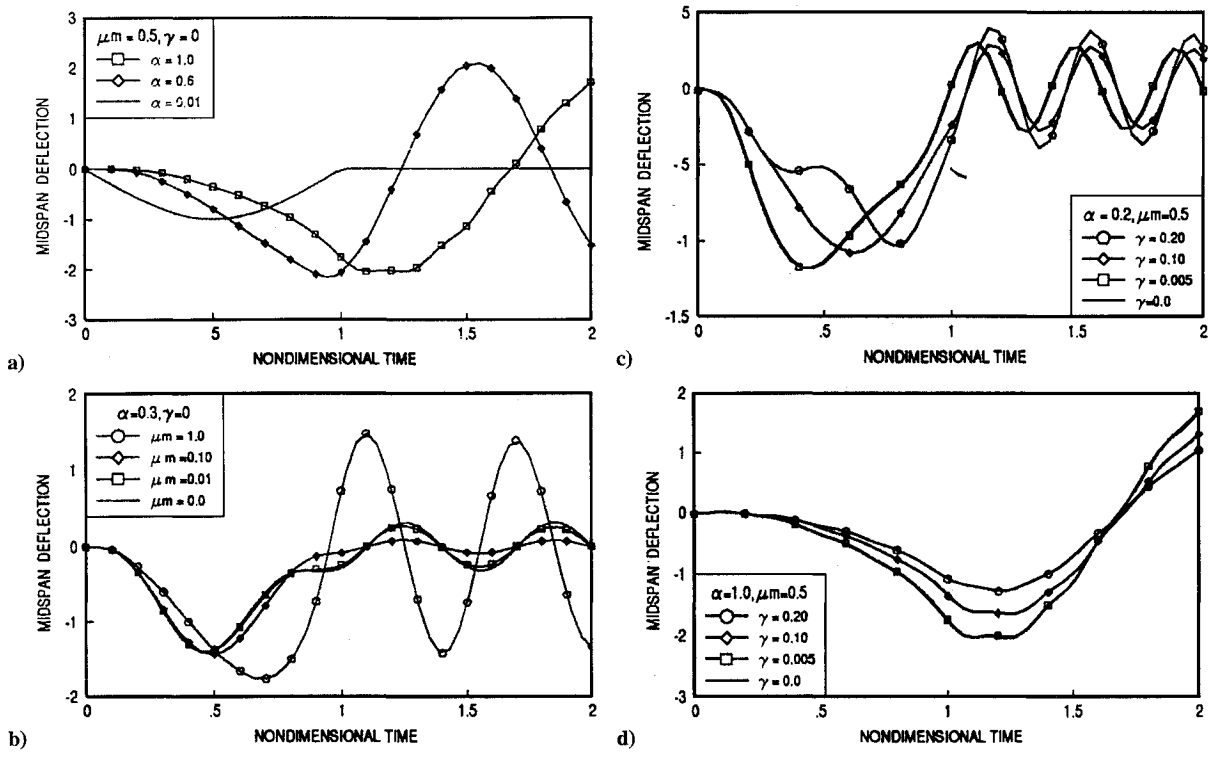

Fig. 3 Vehicle traveling over a flexible beam: pinned-pinned.

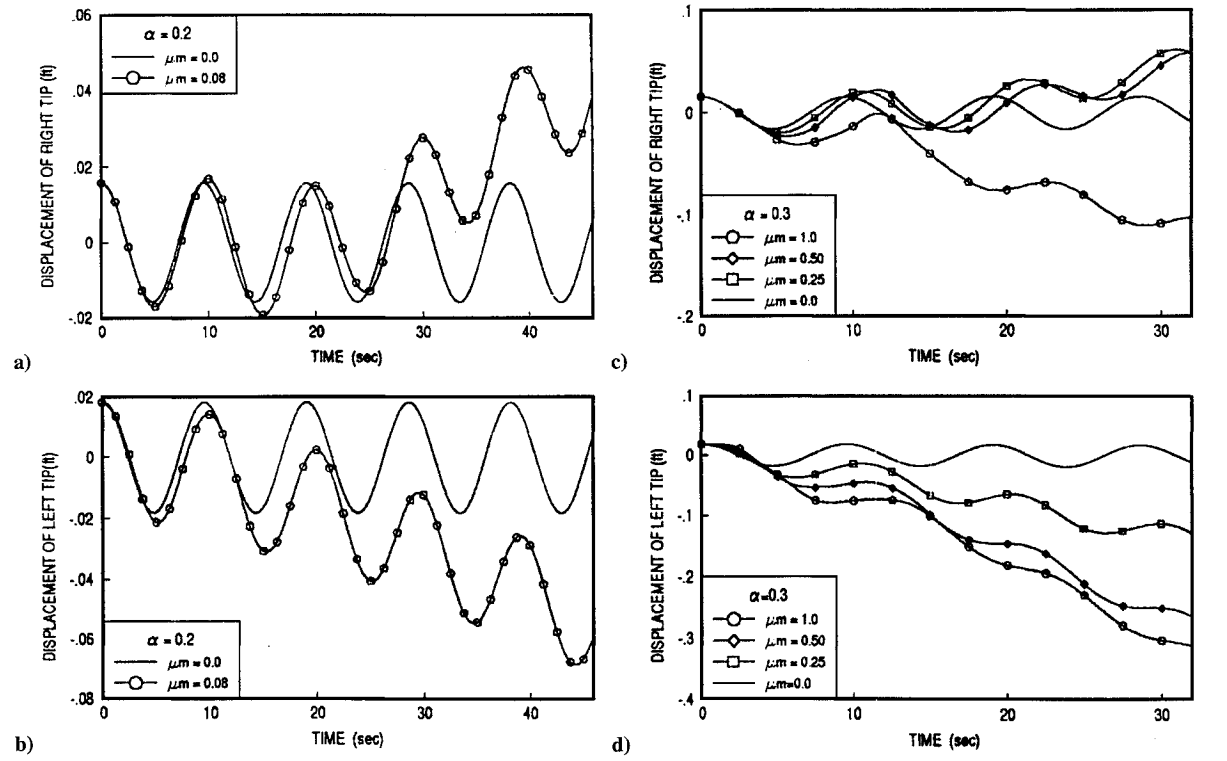

Fig. 4 Vehicle traveling over a planar truss: free-free.

structure. Here l is the length of the structure; x and $w(x, t)$ locate an element of mass along the structure; 1% damping is applied.

To promote ease of interpretation of the results, the following nondimensional parameters are defined.

Time:

$$\tau = t/(v/l) \tag{79}$$

Displacements:

$$\bar{w} = w/l, \qquad \bar{x} = x/l \tag{80}$$

Wheels spacing:

$$\gamma = b/l \tag{81}$$

Speed:

$$\alpha = \pi v/\omega_m l \qquad (v = \dot{s}) \tag{82}$$

Mass ratio:

$$\mu_m = m_m/\rho l \tag{83}$$

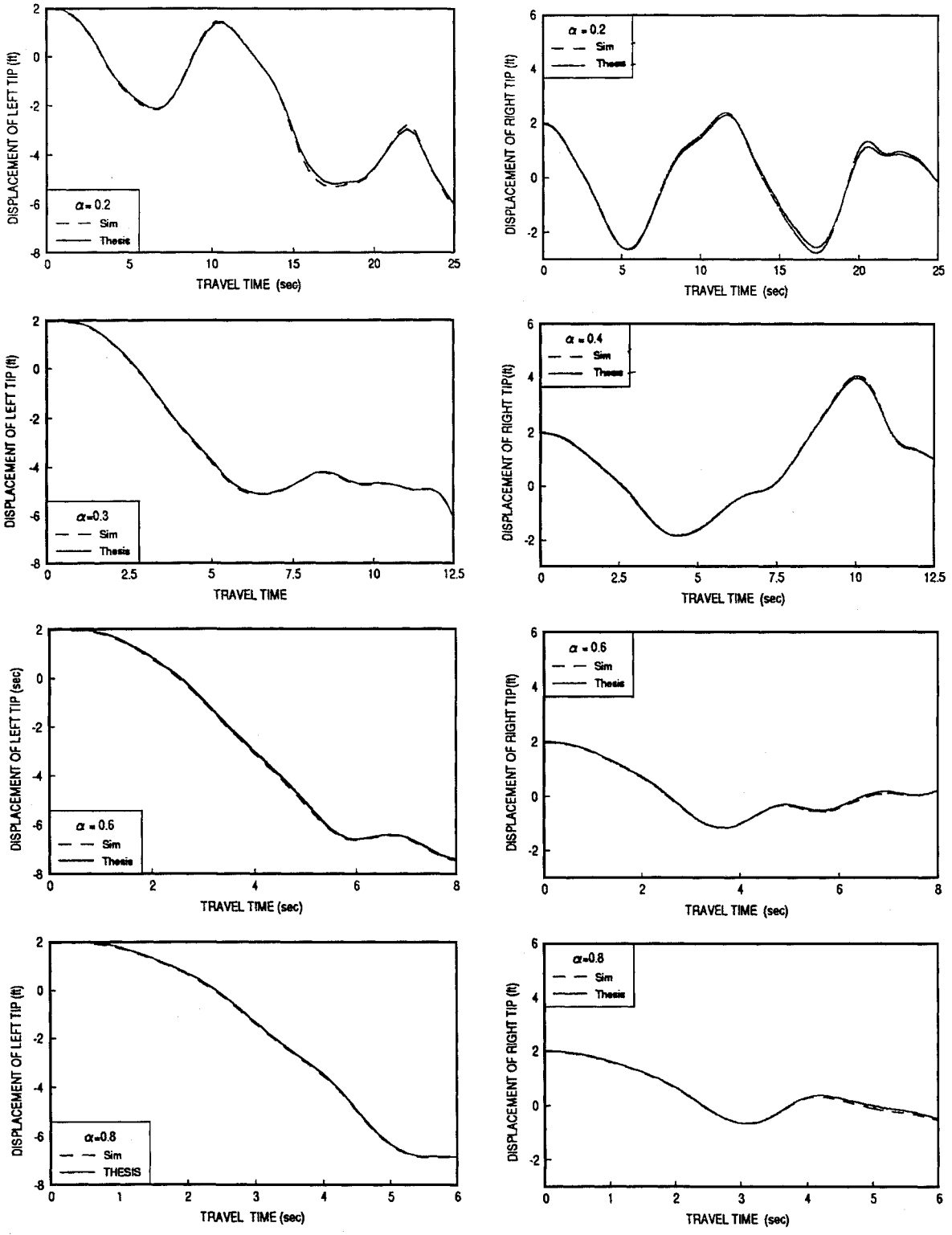

Fig. 5 Point-mass moving over a flexible beam, $\mu m = 0.5$, or a planar truss: free-free.

In the preceding equations, the following definitions apply: ω_1 is the beam fundamental frequency and m_m the moving mass. Note that the preceding nondimensionalization scheme is not unique. It merely offers variables that lend themselves to ready physical interpretation. For example, the speed parameter equals one when the travel time equals half the fundamental period.

The planar truss (Fig. 2b) is 100 ft long, has a mass of 65,000 lbm, is made of aluminum, and has a fundamental frequency of 0.66 rad/s. In the case of the truss, a point mass travels at constant speed. Note that the characteristics of the truss are such that its dynamics behavior will be similar to those of an equivalent beam, thereby facilitating comparison with previously published results.

B. Results

Numerical results are presented in Figs. 3–5. Figure 3 presents results for example 1 and Fig. 4 for example 2. In Fig. 5, the behavior of example 2 is compared to that of the space beam of Ref. 13.

Figure 3 displays the behavior of example 1, where gravity forces are present. When the wheel-spacing parameter γ vanishes, example 1 finds reference points in Refs. 1, 4, and 13. The results presented agree completely with those of these references. As the parameter γ becomes nonzero, the curves expectedly separate (see Figs. 3c and 3d). Figures 3a and 3b display the impact of varying the speed and mass parameters, respectively. Results are shown for two distinct values of the speed parameter (α).

The dynamics behavior for example 2 is displayed in Fig. 4. The truss is assumed initially deformed according to its first free-free mode. Then a point mass travels at constant speed on the truss. The behavior observed is intuitively satisfactory. As can be seen, when the mass-ratio parameter vanishes, free sinusoidal vibration of the first mode prevails (Figs. 4a–4d). As the point-mass magnitude increases, the left (Fig. 4b) and right (Fig. 4a) truss tips behave in nearly asymmetrical fashion (for a speed parameter of 0.2). Figures 4c and 4d display the behavior of the left and right tips as the mass parameter increases, for speed parameter of 0.4.

Further validation of the analytical development is obtained by generating results that could be compared against those published in Ref. 13. Figure 5 shows good comparison between beam[13] and truss results. The Ref. 13 results were obtained using a purely continuous-space-domain approach. That is, the displacement field was expressed in terms of a linear combination of continuous functions. The minor differences in the curves occur because a beam only approximates the behavior of a truss. The interested reader will also find results for discrete beam in Ref. 13, using a degenerate case of the present analysis.

VI. Conclusions

This paper presented a general dynamics modeling approach for flexible-body contact problems. A general mathematical framework for modeling contact kinematics is employed for obtaining a comprehensive set of governing dynamics equations. Explicit expressions for the contact constraint are developed for the case involving two flexible bodies moving relative to each other along a rectilinear track. The development of this particular case is motivated by the dynamics problem posed by the SSMT. A model reduction approach has been presented, which renders this methodology applicable to large structural systems. Numerical results are provided in a variety of cases.

References

[1]Cifuentes, O. A., "Dynamic Response of a Beam Excited by a Moving Mass," *Finite-Element in Analysis and Design*, Vol. 5, Elsevier Science, Amsterdam, 1989, pp. 237–246.

[2]Taheri, M., and Ting, E., "Dynamic Response of Plate to Moving Loads: Structural Impedance Method," *Computers and Structures*, Vol. 33, No. 6, 1989, pp. 1379–1393.

[3]Kurihara, M., and Shimogo, T., "Vibration of an Elastic Beam Subjected to Discrete Moving Loads," *Journal of Mechanical Design*, Vol. 100, July 1978, pp. 514–519.

[4]Yoshida, D., and Weaver, W., "Finite-Element Analysis of Beams and Plates with Moving Loads," *Publication International Association of Bridge Structure Engineering*, Vol. 31, No. 1, 1971, pp. 179–195.

[5]Bodley, C., Devers, D., and Park, C., "A Digital Computer Program for the Dynamic Interaction Simulation of Controls and Structure (DISCOS)," Vol. 1, NASA TP 1219, May 1978.

[6]Nanda, S., "ADAMS Completion and Its Applications," Queen's Univ., Kingston, ON, Canada, 1979.

[7]Anon., "DADS Reference Manual," Computer-Aided Design Software, Inc., July 1989.

[8]Anon., "Applications Manual," MacNeal Schwendler Corp., MSC/NASTRAN, Los Angeles, CA, Sec. 2.14.

[9]Bathe, K., "ADINA: A Finite-Element Program for Automatic Dynamic Incremental Non-Linear Analysis," Acoustics and Vibration Lab., Mechanical Engineering Dept., Massachusetts Inst. of Technology, Cambridge, MA, 1977.

[10]Dailey, G., Caywood, W., and O'Connor, J., "A General-Purpose Computer Program for the Dynamic Simulation of Vehicle-Guideway Interactions," *AIAA Journal*, Vol. 11, No. 3, 1973, pp. 278–282.

[11]Gockel, M. A., "Handbook for Dynamics Analysis," MacNeal–Schendler Corp., MSC/NASTRAN Vers. 63, Los Angeles, CA, June 1983, pp. 3.5-9–3.6-2.

[12]Craig, R. R., and Bampton, C. M., "Coupling of Structures for Dynamics Analyses," *AIAA Journal*, Vol. 6, No. 7, 1968, pp. 1313–1319.

[13]Herman, D., "Discrete and Continuous Dynamics Modeling of a Mass Moving on a Flexible Structure," M.S. Thesis, Dept. of Aeronautics and Astronautics, Massachusetts Inst. of Technology, Cambridge, MA, Feb. 1992.